A MODEL FOR THE PREDICTION OF FIBRE-MATRIX DEBOND INITIATION UNDER MULTIAXIAL STATIC LOAD

P. A. Carraro*, M. Quaresimin

Department of Management and Engineering, University of Padova, Str.la S. Nicola 3, Vicenza, Italy
**carraro@gest.unipd.it*

Keywords: Finite Fracture Mechanics, Debonding, Multiaxial

Abstract
In the present work a model is proposed to predict the onset of a fibre-matrix debond crack for a fibre embedded in an infinite plate and subjected to combined transverse and anti-plane shear stresses. The model is based on the Finite Fracture Mechanics approach, which combines a stress and an energy criterion as necessary conditions for failure. A parametric analysis is carried out in order to understand the influence of the main geometrical and interface parameters on the critical debonding stress under multiaxial static loading. In particular, the critical stress is found to increase when the fibre radius is decreased. The model is validated against experimental results from the literature on off-axis single-fibre-composites and a good agreement is found. As a consequence, the model, suitably adapted, could represent a useful tool for improving the understanding and the quantitative description of the onset of damage in off-axis laminae under static loading.

1. Introduction

Fibre-matrix debonding is one of the most important damage mechanisms leading to the static and fatigue failure of composite laminae under off-axis loading. Some papers in the literature report results on the influence of fibres sizing on the static strength under transverse load [1-2], also combined with in-plane shear [3]. These results prove that the initiation and propagation of debond cracks, affected by the fibres surface treatments, are fundamental mechanisms in the static failure process for off-axis laminae. For this reason this phenomenon has received quite a large attention in the last decades, mainly focusing on the propagation of cracks already existing at the fibre-matrix interface. Toya [4] presented close form expressions for the stress and displacement fields for an arc crack at the interface of a fibre embedded in an infinite plate under remote transverse tension. Chao and Huang instead obtained the stress distributions in the case of anti-plane shear load [5]. Toya's equations were adopted in Refs. [6,7] for analysing the longitudinal propagation of a debond crack and by Paris and co-authors [8] to treat the problem of circumferential propagation and kinking out of the interface.
Concerning the debonding initiation phenomenon, experimental tests were carried out by Ogihara and Koyanagi [9] on cruciform single fibre composites under off-axis load, causing the presence of local radial and shear stresses at the interface. The authors presented the results in the radial-shear stresses plane providing a fitted quadratic expression for the failure locus under a combination of these two stress components.

The main limit of a stress-based criterion is that it does not account for the scale effect, since stress fields are independent of the fibre's radius. Under this point of view, Cohesive Zone Models (CZMs), as those adopted by Chandra [10] and Koyanagi [11] have the advantage that they combine a stress and an energy criterion, thus being sensitive to the fibre dimension.
Another approach which combines a stress and an energy criterion is the Finite Fracture Mechanics (FFM) approach, initially proposed by Leguillon [12] as a general approach to predict failure initiation in conditions in which the classical mechanics and the linear elastic fracture mechanics fail or cannot be applied. This approach was adopted by Mantič et al. [13] to predict the initiation of a debond crack for a fibre embedded in an infinite plate under remote transverse stress. In this work the FFM approach is used as the basis to develop a debond initiation criterion in the case of a fibre in an infinite plate under combined remote transverse and anti-plane shear stresses. This combination of stresses is representative of the local multiaxial condition arising in off-axis plies under uniaxial load.

2. Problem definition and approach

Let us consider the case of an isotropic fibre of infinite length and radius R_f embedded in an infinite matrix plate, as shown in figure 1a. The remote transverse and anti-plane shear stresses (σ_x and σ_{xz}) are named σ_2 and σ_6, respectively, to emphasise their correspondence with the in-plane transverse and shear stresses for composite laminae. The parameter $\lambda_{12} = \sigma_6/\sigma_2$ is used to quantify the degree of multiaxiality of the remote stresses.

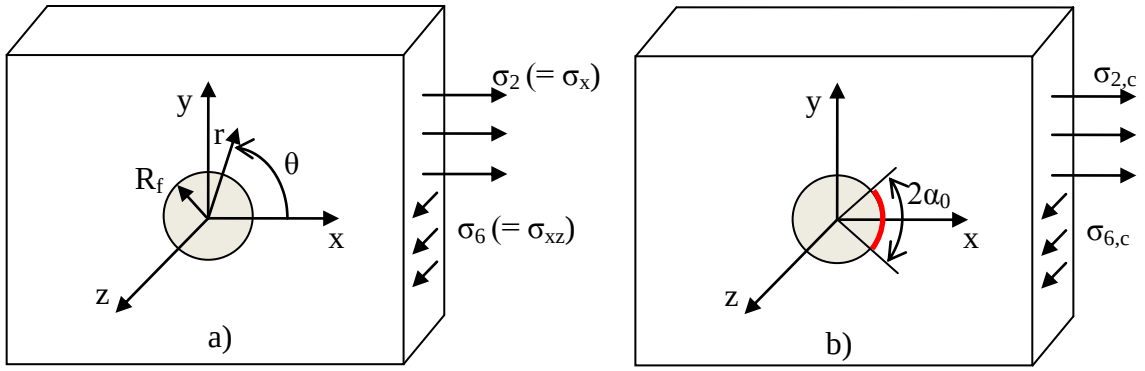

Figure 1: Fibre embedded in an infinite plate with a) pristine and b) partially debonded interface

The FFM approach is based on the idea that the onset of an interface crack occurs with a finite crack angle $2\alpha_0$ (figure 2b). This angle is, together with the critical nominal stress for crack initiation $\sigma_{2,c}$, an unknown of the problem. These two unknowns can be calculated by solving simultaneously the following system of equations, representing the stress and energy conditions required for the crack initiation to occur.

$$\begin{cases} \sigma\left(\sigma_2, \alpha, \lambda_{12}\right) = \sigma_R & (1.1) \\ \Delta G\left(\sigma_2, \alpha, \lambda_{12}\right) = G_c & (1.2) \end{cases}$$

Equation (1.1) represents the stress criterion, which states that the stress along the length of the nucleated crack has to be at least equal to the static strength σ_R of the bi-material interface. Equation (1.2) represents, instead, the energy criterion, which requires that the energy released in the initiation process of a crack of finite angle 2α, divided by the crack area, ΔG,

has to be at least equal to the critical value of the Strain Energy Release Rate (SERR), G_c. The latter is a material property which could be better interpreted as the specific energy necessary for the formation of new crack surfaces.
The simultaneous solution of equations (1.1) and (1.2) allows one to determine the value of the critical remote transverse stress $\sigma_{2,c}$, and the finite angle of the nucleated defect α_0, as functions of the biaxiality ratio λ_{12}.
In order to solve the governing system, the interface stresses and the relative crack faces displacements have to be calculated for the uncracked and cracked conditions, respectively, both under pure transverse and anti-plane shear stress. In addition, the material properties G_c and σ_R have to be known. The latter should be ideally measured by means of a tensile test of the bi-material system in a condition where the stress criterion holds, i.e. testing specimens large enough, as discussed later on in section 7. From this point of view the test method proposed in Ref. [14] could be a useful tool for measuring the bi-material interface strength under normal and shear stress. The critical SERR G_c can instead be obtained by means of the analysis of the mode I propagation of a crack at the considered bi-material interface.

3. Stress fields for the uncracked case

As shown in Refs. [15,16], the stress fields at the fibre-matrix interface ($r = R_f$) under remote transverse stress and anti-plane shear are given in equations (2)-(4).

$$\sigma_r = \sigma_2 \cdot \mu_1 (1+\kappa_2)\left[\frac{1}{4\mu_1 + 2\mu_2(\kappa_1 - 1)} + \frac{Cos(2\theta)}{2(\kappa_2\mu_1 + \mu_2)}\right] \tag{2}$$

$$\tau_{r\theta} = -\sigma_2 \cdot Sin(2\theta)\frac{\mu_1(1+\kappa_2)}{2(\kappa_2\mu_1 + \mu_2)} \tag{3}$$

$$\tau_{rz} = \sigma_6 \cdot Cos(\theta)\cdot\left(1 + \frac{\mu_1 - \mu_2}{\mu_1 + \mu_2}\right) \tag{4}$$

Subscripts 1 and 2 refer to the fibre and the matrix, respectively. θ is the polar angle shown in figure 1a), μ_i is the shear modulus and $\kappa_i = 3 - 4\nu_i$, ν_i being the Poisson's ratio of the material. The angle θ_0 is defined as the angular coordinate where the radial stress vanishes ($\sigma_r(\theta_0) = 0$), and it is about 66° for the material system under investigation. It is worth mentioning that the analysis is restricted to the stress components which can provoke debonding.

4. Displacements fields for the cracked case

The relative crack face displacements in the case of a remote transverse stress have been determined by Toya [4] by means of the complex potential method. The final expressions for the relative displacements Δu and Δv in the radial and tangential direction are reported in equations (5) and (6).

$$\Delta u(\alpha,\theta) = -\frac{\sigma_2}{2} \times A \times R_f \times \left(h_1(\alpha,\theta) \times r_1(\alpha,\theta) + h_2(\alpha,\theta) \times r_2(\alpha,\theta)\right) \tag{5}$$

$$\Delta v(\alpha,\theta) = -\frac{\sigma_2}{2} \times A \times R_f \times \left(h_2(\alpha,\theta) \times r_1(\alpha,\theta) - h_1(\alpha,\theta) \times r_2(\alpha,\theta)\right) \tag{6}$$

The functions $h_i(\alpha,\theta)$ and $r_i(\alpha,\theta)$ are given in Ref. [16], while

$$A=\frac{k}{4}\times\left(\frac{1+\kappa_2}{\mu_2}+\frac{1+\kappa_1}{\mu_1}\right),\ \eta=\frac{\mu_1+\kappa_1\mu_2}{\mu_2+\kappa_2\mu_1},\ \beta=\frac{\mu_2(1+\kappa_1)}{\mu_2+\kappa_2\mu_1},\ \lambda=-\frac{\ln\eta}{2\pi},k=\frac{\beta}{1+\eta} \tag{7}$$

It is worth mentioning that, for high crack angles, the relative radial displacements predicted by equation (5) become negative in proximity of the crack tips, thus predicting an unrealistic interpenetration between the two phases. As a consequence, equation (5) can be considered reliable until the interpenetration zone is very small. In the present work the maximum allowable extension of this region is set equal to 1°. Equations (5,6) can therefore be used for crack angles lower than a limit value $2\alpha_\ell$ which is found to be approximately equal to 140 degrees for a typical glass/epoxy system. An exact description of the displacement field should consider the contact between fibre and matrix, but in the present work this aspect is not treated, this being not restrictive for the model developed. In fact the limit angle α_ℓ (70°) is greater than θ_0 (66°), for which the interface radial stress goes to zero and then becomes negative. The influence of a compressive radial contribution on the debond initiation is not treated in this work and therefore the actual limit angle for the applicability of the present model is equal to $\theta_0 < \alpha_\ell$.
The relative displacements fields in the *z*-direction, Δw, in the case of anti-plane shear were obtained in Ref. [16] from the stress fields presented in [5]. They read as

$$\Delta w(\alpha,\theta)=\sigma_6\cdot R_f\cdot\sqrt{2}\,\frac{\mu_1-2\mu_2}{\mu_2(\mu_2+\mu_1)}Cos\left(\frac{\theta}{2}\right)\sqrt{Cos(\theta)-Cos(\alpha)} \tag{8}$$

5. Calculation of the released energy

Once the interface stresses and the relative displacements are known for the pre and post-debonding conditions respectively, the energy released during the initiation process ΔU can be calculated as follows.

$$\Delta U_I=\frac{1}{2}R_f\int_{-\alpha}^{\alpha}\sigma_r\cdot\Delta u\ d\theta \tag{9}$$

$$\Delta U_{II}=\frac{1}{2}R_f\int_{-\alpha}^{\alpha}\tau_{r\theta}\cdot\Delta v\ d\theta \tag{10}$$

$$\Delta U_{III}=\frac{1}{2}R_f\int_{-\alpha}^{\alpha}\tau_{rz}\cdot\Delta w\ d\theta \tag{11}$$

The subscripts I, II and III highlight that the three contributions are related to mode I, mode II and mode III loading, respectively. Thanks to the solutions given in sections 3 and 4, the energy contributions can be written as functions of the crack angle:

$$\Delta U_I(\alpha)=\sigma_2{}^2\cdot R_f^2\cdot\Omega_p\cdot I_1(\alpha) \tag{12}$$

$$\Delta U_{II}(\alpha)=\sigma_2{}^2\cdot R_f^2\cdot\Omega_p\cdot I_2(\alpha) \tag{13}$$

$$\Delta U_{III}(\alpha)=\sigma_6{}^2\cdot R_f^2\cdot\Omega_a\cdot I_3(\alpha) \tag{14}$$

where Ω_p and Ω_a are non-dimensional parameters defined as

$$\Omega_p=\frac{1}{2}A\cdot\mu_1(1+\kappa_2),\quad \Omega_a=2\sqrt{2}\,\frac{\mu_1(\mu_1-2\mu_2)}{\mu_2(\mu_1+\mu_2)} \tag{15}$$

and

$$I_1(\alpha) = -\int_o^{\alpha} \left(h_1(\alpha,\theta)\cdot r_1(\alpha,\theta) + h_2(\alpha,\theta)\cdot r_2(\alpha,\theta) \right) \left(\frac{Cos(2\theta)}{2(\kappa_2\mu_1+\mu_2)} + \frac{1}{4\mu_1+2\mu_2(\kappa_1-1)} \right) d\theta \qquad (16)$$

$$I_2(\alpha) = \frac{1}{2(\kappa_2\mu_1+\mu_2)} \int_o^{\alpha} \left(h_2(\alpha,\theta)\cdot r_1(\alpha,\theta) - h_1(\alpha,\theta)\cdot r_2(\alpha,\theta) \right) Sin(2\theta)\, d\theta \qquad (17)$$

$$I_3(\alpha) = \frac{1}{\mu_1+\mu_2} \int_0^{\alpha} Cos(\theta)\cdot Cos\left(\frac{\theta}{2}\right) \sqrt{Cos(\theta)-Cos(\alpha)}\; d\theta = \\ = \frac{\sqrt{2}\pi}{16(\mu_1+\mu_2)} \left(1-Cos(\alpha)\right)\left(Cos(\alpha)+3\right) \qquad (18)$$

A closed form solution was obtained for I_3, whereas I_1 and I_2 were computed numerically by means of a simple trapezoidal rule with integration steps of 1°.

6. Solution of coupled stress and energy criteria

When transverse and anti-plane stresses are simultaneously applied, three interface stress components σ_r, $\tau_{r\theta}$ and τ_{rz}, are responsible for debond initiation. As a consequence an equivalent stress, σ_{eq}, should be defined to be used in the stress criterion, as in equation (19).

$$\sigma_{eq} = \sqrt{\sigma_r^2 + c\cdot\left(\tau_{r\theta}^2 + \tau_{rz}^2\right)} \qquad (19)$$

c is a constant equal to the square of the ratio between the normal and shear strength of the bi-material interface. The analysis of SiC/Ti and glass/epoxy systems [10,11] proved that a value of *c* about unity provides good results if the stress criterion is coupled with an energy criterion by means of a CZM. A value close to 1 was experimentally found in [14] for an aluminium/epoxy system. However the value of this constant is still an open problem.
Concerning the energy criterion, in a biaxial loading condition the total SERR can be calculated dividing the total released energy by the area of the nucleated crack, $2A_c$:

$$\Delta G = \frac{\Delta U_{tot}}{2A_c} = \frac{\Delta U_I + \Delta U_{II} + \Delta U_{III}}{2\alpha\cdot R_f} \qquad (20)$$

Therefore, the energy criterion, equation (1.2), can be explicitly rewritten as follows:

$$\Delta U_{tot} = 2\alpha\cdot R_f\cdot G_c \qquad (21)$$

It is clear that the released energy is the sum of the contributions due to mode I, II and III loadings. A detailed discussion was reported by the authors in Ref. [16] to support the fact that the critical SERR, G_c, has to be considered constant, different from what was proposed by Mantič and co-authors [13].
Eventually the governing system of two equations, representing the stress and energy criteria, can be explicitly written as follows.

$$\begin{cases} \sigma_r^2\left(\sigma_2,\alpha\right)+c\left[\tau_{r\theta}^2\left(\sigma_2,\alpha\right)+\tau_{rz}^2\left(\lambda_{12}\sigma_2,\alpha\right)\right]=\sigma_R^2 & (22.1) \\ \sigma_2^2\cdot R_f\left[\Omega_p\cdot\left(I_1\left(\alpha\right)+I_2\left(\alpha\right)\right)+\lambda_{12}^2\cdot\Omega_a\cdot I_3\left(\alpha\right)\right]=2\alpha\cdot G_c & (22.2) \end{cases}$$

In equation (22.1) it is emphasised that the local stresses at the interface are functions of the angle α, the remote stress σ_2, which are unknown variables, and the biaxiality ratio λ_{12}.
As α is involved in complicated expressions within the integrals $I_{1,2,3}(\alpha)$, a closed form solution for the system cannot be provided. However the value of $\sigma_{2,s}$ and $\sigma_{2,e}$ satisfying the stress and energy criteria, respectively, can be calculated as a function of the crack angle α from equations (22.1) and (22.2):

$$\sigma_{2,s}\left(\alpha\right)=\frac{\sigma_R}{\sqrt{k_{rr}(\alpha)^2+c\left(k_{r\theta}(\alpha)^2+\lambda_{12}^2\cdot k_{rz}(\alpha)^2\right)}} \quad (23.1)$$

$$\sigma_{2,e}\left(\alpha\right)=\sqrt{\frac{G_c}{R_f}\cdot\frac{2\alpha}{\left[\Omega_p\cdot\left(I_1\left(\alpha\right)+I_2\left(\alpha\right)\right)+\lambda_{12}^2\cdot\Omega_a\cdot I_3\left(\alpha\right)\right]}} \quad (23.2)$$

The terms $k_{ij}(\alpha)$ in equation (23.1) are the interface stress concentration factors at the angle θ=α with respect to the *x*-axis. They can be easily obtained dividing equations (2), (3) and (4) by the remote stresses σ_2 and σ_6.

$$k_{rr}\left(\alpha\right)=\mu_1\left(1+\kappa_2\right)\left[\frac{1}{4\mu_1+2\mu_2\left(\kappa_1-1\right)}+\frac{Cos\left(2\alpha\right)}{2\left(\kappa_2\mu_1+\mu_2\right)}\right] \quad (24)$$

$$k_{r\theta}\left(\alpha\right)=-Sin\left(2\alpha\right)\frac{\mu_1\left(1+\kappa_2\right)}{2\left(\kappa_2\mu_1+\mu_2\right)} \quad (25)$$

$$k_{rz}\left(\alpha\right)=Cos\left(\alpha\right)\left(1+\frac{\mu_1-\mu_2}{\mu_1+\mu_2}\right) \quad (26)$$

The initial angle α_0 can be computed equating equations (23.1) and (23.2), resulting in equation (27) to be solved numerically for α_0.

$$\frac{\frac{1}{2\alpha_0}\left[\Omega_p\cdot\left(I_1\left(\alpha_0\right)+I_2\left(\alpha_0\right)\right)+\lambda_{12}^2\cdot\Omega_a\cdot I_3\left(\alpha_0\right)\right]}{k_{rr}(\alpha_0)^2+c\left(k_{r\theta}(\alpha_0)^2+\lambda_{12}^2\cdot k_{rz}(\alpha_0)^2\right)}=\frac{1}{R_f}\frac{G_c}{\sigma_R^2} \quad (27)$$

Once the initial angle has been calculated, the critical remote transverse stress can be easily computed by substituting α_0 in equation (23.1) or (23.2).
Thus, the solution depends on the fibre radius R_f, on the interface toughness G_c and strength σ_R, as well as on the biaxiality ratio λ_{12}. A new interface parameter is defined as follows.

$$\Gamma=\frac{1}{R_f}\frac{G_c}{\sigma_R^2} \quad (28)$$

The dimension of Γ is MPa^{-1} when R_f, G_c and σ_R are expressed in mm, kJ/m^2 and MPa, respectively.

7. Parametric analysis, validation and conclusions

According to equation (27) the initial angle α_0 depends only and directly on the interface parameter Γ. Let us consider first the case $c = 0$. The trend of the initial angle as a function of Γ is shown in figure 2a. It was proved in Ref. [16] that when Γ tends towards zero, α_0 approaches zero as well. This means that, when $\Gamma \to 0$, applying the FFM approach is equivalent to apply a point stress criterion at the fibre pole. In fact, figure 2b shows that the remote transverse stress predicted by the coupled criteria tends asymptotically to the value obtained by the stress criterion only (equation (23.1)). This happens when R_f is very large or the G_c to σ_R^2 ratio is very small. This confirms why testing large enough specimens allows one to determine the bi-material strength σ_R to be used in the stress criterion, as mentioned in section 2. Conversely, if Γ tends towards infinity (R_f is very small or the G_c to σ_R^2 ratio is very high), α_0 approaches the angle θ_0 for which the radial stress vanishes. In this conditions the angle is not a variable of the problem, and the critical stress tends towards the one which satisfies the energy criterion only, which has a linear dependence on $\Gamma^{0.5}$, as shown in figure 3b. When $c = 0$ the influence of λ_{12} is appreciable only if Γ does not approach zero.

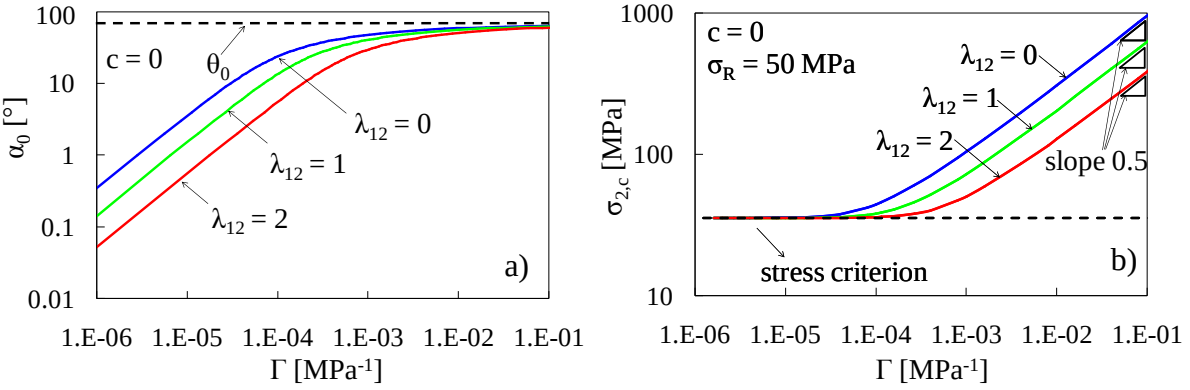

Figure 2: a) initial angle and b) critical remote transverse stress against Γ for glass/epoxy

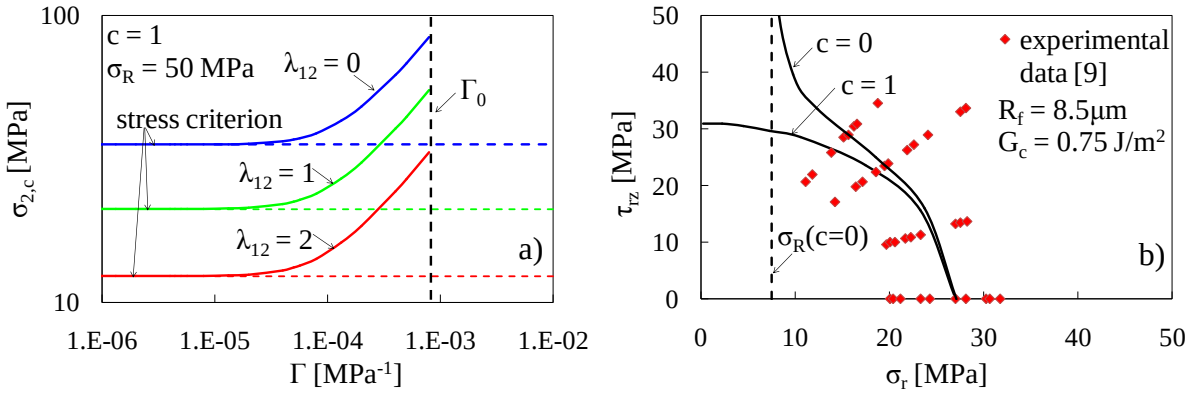

Figure 3: a) Critical remote transverse stress against Γ for $c = 1$ and glass/epoxy system; b) comparison between model predictions and experimental data from [9]

Conversely, if c is higher than zero, the biaxiality ratio affects also the solution relevant to the stress criterion, as shown in figure 3a for $c = 1$. In such a case, as discussed in Ref. [16], the analysis has to be limited to a maximum value of Γ equal to

$$\Gamma_0 = \frac{\Omega_a \cdot I_3(\theta_0)}{2\theta_0 \cdot c \cdot k_{rz}(\theta_0)} \tag{30}$$

The model is eventually validated against the experimental results presented in [9]. The value of σ_R was calibrated on the experimental results for the pure transverse stress case, while a value of G_c equal to 0.75 J/m^2 was chosen on the basis of comparisons with other results from the literature, as better explained in Ref. [16]. Two values of *c* were considered (0 and 1) and both predictions are in good agreement with experimental data, as shown in figure 3b. At present it is difficult to say which choice for the parameter *c* is more appropriate.

References

[1] S. Keusch, H. Queck, K. Gliesche , Influence of glass fibre/epoxy resin interface on static mechanical properties of unidirectional composites and on fatigue performance of cross ply composites. *Compos Part A-Appl S*, 29(A): 701-705, 1998.

[2] J. M. M. De Kok, T. Peijs, Deformation, yield and fracture of unidirectional composites in transverse loading 2. Influence of fibre-matrix adhesion, *Compos Part A-Appl S*, 30: 917-932, 1999.

[3] F. Hoecker, K. Friedrich, H. Blumberg, J. Karger-Kocsis, Effect of fiber/matrix adhesion on off-axis mechanical response in carbon-fiber/epoxy resin composites. *Compos Sci Technol*, 54: 317-327, 1995.

[4] M. Toya, A crack along a circular inclusion embedded in an infinite solid. *J Mech Phys Solids*, 22: 325-348, 1974.

[5] C. H. Chao, W. J. Huang, Antiplane problem of curvilinear cracks in bonded dissimilar materials. *Int J Fracture*, 64: 179-190, 1993.

[6] H. Zhang, M. L. Ericson, J. Varna, L. A. Berglund, Transverse single-fibre test for interfacial debonding in composites: 1. Experimental observations. *Compos Part A-Appl S*, 28A: 309-315, 1997.

[7] J. Varna, L. A. Berglund, M. Ericson, Transverse single fibre test for interfacial debonding in composites: 2 Modelling. *Compos Part A-Appl S*, 28A: 317-326, 1997.

[8] F. Paris, E. Correa, V. Mantič, Kinking of transversal interface cracks between fiber and matrix. *J Appl Mech*, 74: 703-716, 2007.

[9] S. Ogihara, J. Koyanagi, Investigation of Combined Stress State Failure Criterion for Glass Fiber/Epoxy Interface by the Cruciform Specimen Method. *Compos Sci Technol*, 70: 143-150, 2010.

[10] N. Chandra, Evaluation of interfacial fracture toughness using cohesive zone model. *Compos Part A-Appl S*, 33: 1433–1447, 2002.

[11] J. Koyanagi, P. D. Shah, S. Kimura, S. K. Ha, H. Kawada, Mixed-Mode Interfacial Debonding Simulation in Single-Fiber Composite under a Transverse Load. *Journal of Solid Mechanics and Materials Engineering*, 3(5): 796-806, 2009.

[12] D. Leguillon, Strength or toughness? A criterion for crack onset at a notch. *Eur J Mech A-Solid*, 21: 61-72, 2002.

[13] V. Mantič, Interface crack onset at circular cylindrical inclusion under a remote transverse tension. Application of a coupled stress and energy criterion. *Int J Solids Struct*, 46: 1287-1304, 2009.

[14] M. A. K. Chowdhuri, Z. Xia, F. Ju, A new test method for the measurement of normal-shear bonding strength at bi-material interface. *Mech Adv Mater Struc*, 20(7): 571-579, 2013.

[15] J. N. Goodier Concentration of stress around spherical and cylindrical inclusions and flaws. *J Appl Mech*, 55: 39-44, 1933.

[16] P. A. Carraro, M. Quaresimin. Modelling fibre–matrix debonding under biaxial loading. *Compos Part A-Appl S*, 61: 33–42, 2014.